Thin-Film Composite Nanofiltration Membrane: A Study on the Curing Time and Its Performance Evaluation

K. H. Mah[1], H. W. Yussof [1*], M. N. Abu Seman[1], A. W. Mohammad[2]

[a]Faculty of Chemical & Natural Resources Engineering, Universiti Malaysia Pahang, Lebuhraya Tun Razak, 26300 Kuantan, Pahang.

[a]Dept. of Chemical and Process Engineering; Faculty of Engineering and Built Environment, Universiti Kebangsaan Malaysia, 43600 Bangi Selangor.

Abstract

Xylose is the raw material for xylitol production which can be obtained through hydrolysis of agriculture waste. However, the presence of glucose in hydrolysate interferes in the process. Thin-film composite membrane developed through interfacial polymerization (IP) can be tailored for xylose separation through manipulation preparation conditions. In this study, the impact of curing conditions, specifically curing time was investigated on xylose separation. The thin-film composite (TFC) membrane was formed from IP between triethanolamine (TEOA) and tri-mesoyl chloride (TMC) on polyethersulfone support membrane. Attenuated Total Reflection Fourier Transform Infrared (ATR-FTIR) spectroscopy and contact angle measurement were performed to investigate the formation of thin-film. Evaluation of membrane performances, namely pure water flux, permeation flux, and xylose separation factor was used to evaluate the TFC membrane cured at a different time (2, 5, 10, 15, and 20 minutes). A decrease in flux was observed when prolonged the curing time for TFC membrane. A minimum of 5 minutes curing time would be needed for the organic solvent to be evaporated from the membrane at 60 ^{o}C, but 15 minute curing time would have better xylose separation.

Keyword: Nanofiltration, Interfacial Polymerization, Thin-film Composite, Curing Time

1. Introduction

Xylose is mainly found in the hemi-cellulosic fraction of hardwoods and herbaceous materials. Consequently, hydrolysis is employed to break the long chain of hemicellulose into xylose [1,2]. Nonetheless, hydrolysis of hemi-cellulosic biomass also produces glucose, another monosaccharide with a considerable fraction in hydrolysates, in addition to the xylose [3,4]. Hence, separation of these monosaccharides is needed to obtain the pure fraction of a specific monosaccharide. Significantly, commercial nanofiltration membrane has demonstrated the ability to separate xylose and glucose from a xylose-glucose mixture [5], which is later applied in different hemicellulose hydrolysate [6]. In another study, an integrated membrane system using commercial membrane to perform enzymatic process, converting glucose to gluconic acid and followed by separation of xylose from gluconic acid by nanofiltration [7].

TFC membranes have experienced tremendous development since the concept of IP was first introduced in 1965 [8]. In the recent decade, development of TFC membrane through IP has received attention due to the improvement of membrane characteristics such as selectivity and fouling resistance [9]. TFC membrane developed using IP allows properties of both bottom substrate and top barrier film to be individually tailored and optimized to achieve desired separation selectivity and flux rate [10]. The top thin layer produced by IP technique determines the overall solute retention, permeate flux, and, in general, controls the efficiency of the membrane process [11]. Nanofiltration (NF) membranes with ultrathin selective layer prepared using this IP technique is an excellent candidate for producing specially tailored TFC membrane for xylose and glucose separation. Tang et al. [12] had utilized TEOA, an environmentally friendly yet economical monomer in enhancing the performance of the thin-film composite membrane. TEOA belong to the tertiary amino group, where its molecules can be flexibly transferred into quaternary ammonium group through variation of feed pH. This unique property allows the membrane to increase hydrophilicity at lower pH feed, making it suitable for biomass hydrolysate application without additional steps.

Curing in IP removes residual organic solvent from the film to promote additional crosslinking between aqueous monomer and organic monomer forming a denser top selective layer [13]. A study by Rao et al. [14] showed the curing process in IP has a huge impact on the TFC membrane flux and separation performance. Curing process also makes the the polymer chains in the IP layer pack more closely and makes IP reaction more complete, which densify the membrane [15]. Curing in IP relies on the temperature and duration of the film are exposed to. TFC membrane using an organic solvent such as hexane, have increased in flux when exposed to 45–60 ^{o}C but drops off above 75 ^{o}C [13,16]. Hence, the curing temperature near the organic solvent's boiling point is highly favorable due to the

*Corresponding author.
E-mail address : hafizuddin@ump.edu.my

high flux and rejection. Many studies reported the best curing time using hexane as an organic solvent were at 55 seconds [16], 3 minutes [14], 10 minutes [13,17], and 15 minutes [15]. These studies applied monomers such m-phenylene-diamine (MPD) [13,14,16,17] and trimethylene tetramine (TETA) [15] in IP, where the IP process took place in a very short time. Though various curing conditions were reported [13–17], the effect of curing on slow IP, such as TEAO and TMC toward membrane performance has no correlative explanations in detail.

This paper aim to study the effect of curing time on the hydrophilicity and performances of TFC membrane developed through IP of TEOA and TMC on PES support membrane. This paper also aims to correlate the effect of curing time toward each TFC membrane performance, namely, pure water flux, permeation flux, and xylose separation factor. In addition, ATR-FTIR and membrane surface hydrophilicity analysis were done on PES and TFC membranes to observe changes in physical and chemical properties after IP.

2. Experimental

2.1 Materials

The asymmetric commercial PES membrane was purchased from AMFOR Inc. (China) with the commercial name of UF PES50. The membrane has a nominal molecular weight cut-off of 50 kDa and water flux (at 25 ºC , 50 PSI) of 260 LMH. The chemicals used in this study were TEOA (R & M Marketing, Essex, UK), TMC (Alfa Aesar, UK), sodium hydroxide (Merck, Germany), n-hexane (Merck, Germany), xylose (Sigma Aldrich, USA), glucose (Sigma Aldrich, USA), and acetonenitrile (J.T. Baker, USA). All these chemicals were analytical grade with high purity (> 99%), also acetonitrile with High Performance Liquid Chromatography (HPLC) grade.

2.2 Preparation of Thin-Film Composite Membrane

The TFC membrane used in this study was prepared by using conventional IP approach according to previous studies with slight modification [12,18]. Commercial PES membrane was immersed in aqueous solution of 4% (w/v) TEOA dissolved in 1 $\times 10^{-6}$ M sodium hydroxide solution for a period of 30 minutes. The membrane was then drained and immersed in an organic solution of 0.25% (w/v) TMC in pure hexane for a period of 45 minutes. Finally, the TFC membrane was dried in an oven (UF 55, Memmert, USA) at a temperature of 2, 5, 10, 15, and 20 minutes.

2.3 Attenuated Total Reflection Fourier Transform Infrared (ATR-FTIR) spectroscopy

ATR-FTIR spectra were obtained using a Thermo Scientific Nicolet iS-10 FT-IR spectrometer equipped with an Attenuated Total Reflection (ATR) element of Smart iTX AR Diamond and an Omnic 5.1 software. The membrane active layers were pressed tightly against the crystal plate. The TFC membrane and PES membrane were analyzed, with each spectrum averaged from 256 scans collected from 650 to 4000 cm^{-1} at 2 cm^{-1} resolution. The experiments run with air as the background and no baseline or ATR corrections were applied.

2.4 Contact Angle Measurement

The contact angles of all the membranes were measured using contact angle goniometer (JY-82, Chengde testing machine Co. Ltd., China) using the sessile drop method. A glass slide was immersed in pure ethanol for 10 min, rinsed with ultrapure water and then dried before being used as an inert flat surface. The membrane was then placed on top of the glass slide and clipped making sure the surface of the membrane is parallel to the glass flat surface. A dangling droplet of 5 µL of ultrapure water at the end of 'I'-shaped needle was carefully deposited to membrane surface to avoid the effect of falling force by gravity. A static image of the droplet in equilibration with the membrane surface was taken. For ensuring the accuracy, the measurements were performed at five different locations, and then the average value was regard as the final contact angle result.

2.5 Membrane Performance

The performance of membrane was measured by pure water flux (Jw), xylose separation factor (Xxyl) and permeation flux (Jv) based on procedures by previous studies [18,19]. These measurements were performed by permeation experiments of ultrapure water for pure water flux, and model sugar solution for xylose separation factor and permeation flux measurement. Xylose separation factor is a measure of xylose purification from glucose. This factor indicates the change in the permeate composition compared to the original ratio of xylose to glucose in the bulk. A value of 1 implies that no separation between xylose and glucose occurs. While, a value greater than 1 implies a ratio of xylose to glucose is higher in permeate than the original ratio (feed), thus xylose enriched in permeate. A value lower than 1 implies the opposite, where glucose is enriched rather than xylose. Freshly prepared TFC membrane was first subjected to pressure pre-treatment at 4 bar for 10 minutes before any permeation experiment. The first permeation experiment performed on the membrane was permeation of ultrapure water to calculate pure water flux. The membrane is then subjected to another permeation

experiment using model sugar solution to calculate the xylose separation factor and permeation flux.

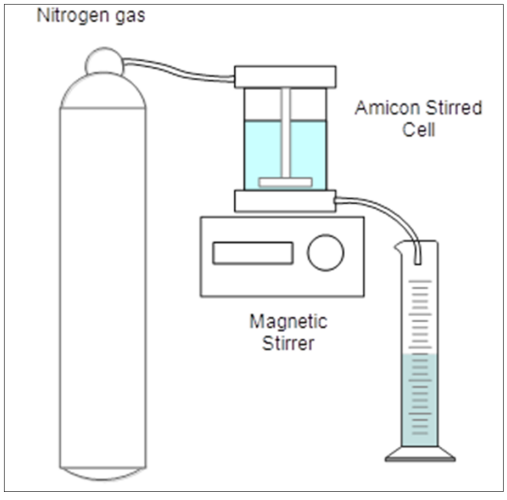

Figure 1 Nanofiltration set-up

2.5.1 Nanofiltration Set-up

A Millipore stirred cell (Model 8200, Millipore-Amicon Corporation, USA) having a maximum volume uptake of 200 mL and an effective membrane area of 2.87 x 10^{-3} m^2 was used in all experiments. Prepared TFC membrane was fitted into the membrane holder at the bottom of the stirred cell. Other parts are then assembled together and place on top of a magnetic stirrer (Model MS-20D, Daihan Scientific Co. Ltd., South Korea). The stirred cell contain a magnetic stirrer to maintain fluid motion during operation to reduce concentration polarization. Ultrapure water or model sugar solutions were filled into the stirred cell. The pressure within the cell was provided by the attached nitrogen cylinder and continuously monitored by the pressure gauge on the cylinder.

2.5.2 Pure Water Flux

Pure water flux was performed by measuring the time taken for 20 mL of ultrapure water collected at 4 bar with the constant stirring speed of 300 rpm. The pure water flux can be calculated using the following equation:

$$J_w = \frac{\Delta V}{A.\,\Delta t} \tag{3}$$

2.5.3 Xylose Separation Factor

180 mL of model sugar solution (5 g/L xylose and 5 g/L glucose) was filled into the stirred cell. The nanofiltration was performed by collecting 20 mL of permeate at pressure 4 bar and stirring speed of 300 rpm at room temperature. The solution of the feed, permeate, and retentate (solution left in stirred cell) were quantified using HPLC. The xylose separation factor is calculated using Eq. (4), slightly modified from Sjoman et al. [5].

$$X_{xyl} = \frac{C_{p\_xyl}/C_{p\_glu}}{C_{b\_xyl}/C_{b\_glu}} = \frac{1-R_{obs\_xyl}}{1-R_{obs\_glu}} \tag{4}$$

where,

$$C_b = \frac{C_f + C_r}{2} \tag{5}$$

$$R_{obs} = 1 - \frac{C_p}{C_b} \tag{6}$$

2.5.4 Permeation flux

The time taken for 20 mL of permeate collected in Section 2.5.3 was used to calculate the permeation flux using the following equation:

$$J_v = \frac{\Delta V}{A.\,\Delta t} \tag{7}$$

2.6 Quantification of Sugar using HPLC

Quantification of samples was done using Agilent's 1200 Series HPLC equipped with refractive index detector. The liquid chromatography column used in this study were Agilent's Zorbax Carbohydrate 5 µm (4.6 × 250 mm) column with its operating flow rate of 1 mL/min and an injection volume of 20 µL. The mobile phase used during analysis was prepared by diluting 3 part for acetonitrile with 1 part of ultrapure water. Prior to any HPLC analysis, the mobile phase was filtered using nylon membrane with pore size of 0.22 µm and degassed using ultrasonic bath at room temperature for 1 hour. All HPLC samples were filtered using a 3 mL syringe with a 0.2 µm filter attached.

3. Results and Discussion

3.1 Interfacial Polymerization

Fig. 2 shows an analysis of the ATR-FTIR spectra for commercial PES membrane (Fig. 2 (a)) used as the support in the preparation of TFC membrane (Fig. 2 (b)). Evaluation on ATR-FTIR spectra in Fig. 2 showed the IP has occurred since two strong bands at 1724 cm^{-1} and 738 cm^{-1} were present in TFC

membrane (Fig. 2 (b)) but absent in PES membrane (Fig. 2 (a)), which belong to functional group of ester ($C = O$ stretch) and alkyl-halides ($C = Cl$ stretch) respectively. The contact angle for PES membrane was 51.0 (±3.7) ° and TFC membranes were in the range between 37.4 (±1.5) ° to 47.0 (±2.0) °. This showed that occurrence of IP also has increases the surface hydrophilicity of the membrane surface. A similar observation has been reported elsewhere, the occurrence of a strong band at 1724 cm^{-1} in spectra [12] and contact angle around 35 ° [20] in TFC membrane from IP between TEOA and TMC.

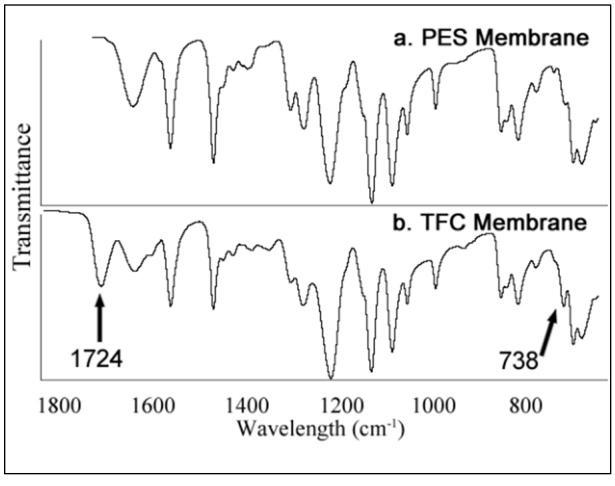

Figure 2 ATR-FTIR Spectra of (a) commercial PES membrane used as a support in preparing (b) TFC membrane

3.2 Effect of Curing Time on Membrane Surface Hydrophilicity

Table 1 gives the summary of all TFC membrane characteristic and performance data for TFC membrane cured with a different period of time (2, 5, 10, 15 and 20 minutes) at 60 °C. The experimental data was then analyzed using Pearson's *r* correlation coefficient to observe any correlation of dependency between two variables linearly as illustrated in Fig. 3. Correlations are classified as high, moderate, and low for coefficients greater than 0.85, between 0.85 and 0.4, and less than 0.4, respectively. It should be noted correlation does not imply causation in general. Curing time has a low negative correlation (r = - 0.37) with contact angle as in Fig. 3 (a), a relative measurement of membrane surface hydrophilicity. Lower contact angle can be relatively associated to higher membrane surface hydrophilicity.

Table 1 Summary of the membrane characteristics and performance at different curing times

Curing Time (minute)	Contact angle (°)	J_w (Lm^{-2} h^{-1})	J_v (Lm^{-2} h^{-1})	X_{xyl}
2	47.0 (±2.0)	15.51 (±1.53)	12.03	1.09
5	40.5 (±1.4)	12.44 (±0.06)	11.12	1.00
10	43.7 (±0.7)	11.42 (±1.09)	9.25	0.97
15	37.4 (±1.5)	9.47 (±0.85)	6.98	1.13
20	43.7 (±4.2)	5.92 (±0.14)	4.79	0.90

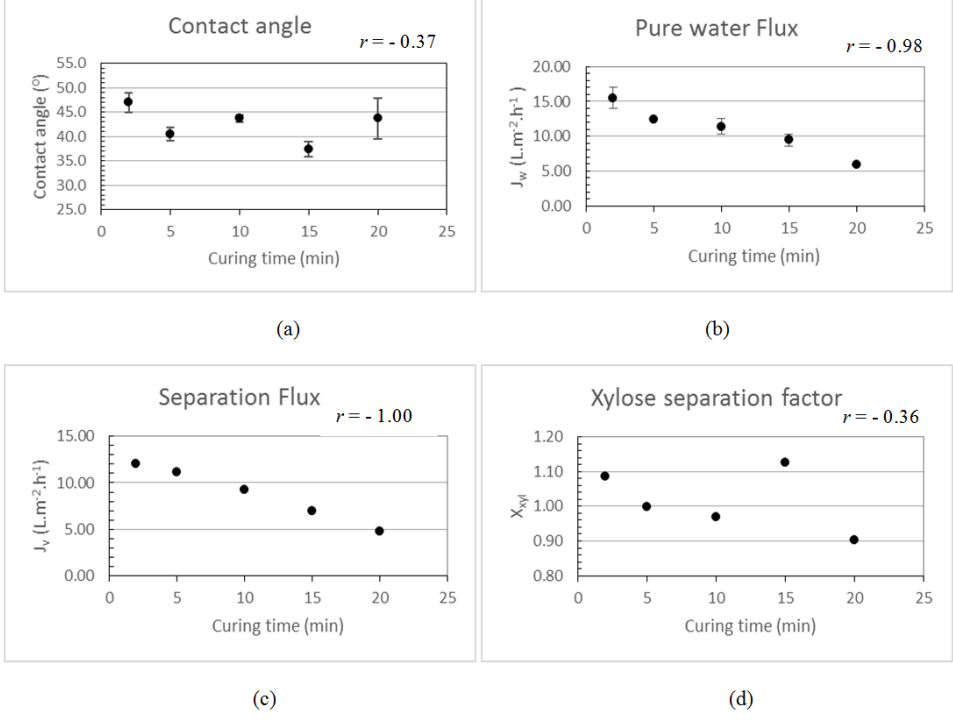

Figure 3 Effect of curing time on (a) contact angle, (b) pure water flux, (c) separation flux, and (d) separation performance

The highest contact angle was measured at 2 minute point which is 47.0 (±2.0) °, from the 5 minute point to 20 minute point were fluctuating between 40-45 ° region before the sudden drop at 15 minute point to 37.4 (±1.5) °. Translating this trending in terms of membrane surface hydrophilicity, as the curing time was prolonged from the 2 minute point onwards, the hydrophilicity of the membrane surface did not improve much except at the 15 minute point. At the 2 minute point, the exposure to the curing temperature was short thus a less dense top layer was formed making it less hydrophilic because of the incomplete removal of solvent from the top layer. This was true when the TFC membrane exit the oven, wetness can be felt in the center of the membrane and also discussed in the previous study by Ghosh et al. [13]. From the 5 minute point onwards, the fluctuation of contact angle implies 5 minutes would be the minimum time for solvents to be evaporated from the film at 60 ºC

3.3 Effect of Curing Time on Membrane Performance

Fig. 3 illustrated the effect of curing on all the membrane performance with their respective correlation coefficient. Curing time has a high negative correlation with pure water flux and permeation flux, where correlation coefficient (*r*) of - 0.98 and - 1.00 were obtained, respectively. Besides, the curing time has a low negative correlation with xylose separation factor with a mere correlation coefficient of - 0.36. The high negative correlation of pure water flux obtained refer to the inverse relationship between curing time with pure water flux. This relationship was also demonstrated in past studies [14,16], where TFC membrane subjected to longer exposure to curing temperature increases the densification of the top layer, causing a decreased in the porosity of the top layer. Hence, the decrease in water flux and permeability.

In another study by [13], a different opinion has been raised where higher permeability was achieved by complete evaporation of organic solvents when subjected to longer curing time. However, prolonging the curing time pass the minimum time needed to remove the solvent also may result in shrinkage or annealing of support membrane pores, which decreases water permeability translating into a decrease in water flux. Further investigation on this matter would be needed to properly explain this phenomenon. However, an improvement in the permeability observed by Ghosh et al. [13] when increasing the curing time did not visualize in this study throughout the curing time studied. This shows explanation by Rao et al. [14] was more relevant in this case.

The inverse relationship between curing time and permeation flux were similar to the one with curing time and pure water flux as discussed previously. In this nanofiltration set-up, the driving force for the transport through the membrane was dominated by pressure gradient across the membrane. Hence, both fluxes have a similar relationship when the curing time was prolonged. As the TFC membrane was subjected to longer exposure to curing temperature, the top layer would become denser which decreases the flux of both water and solute. Although both water flux and permeation flux have an almost similar relationship, attention should draw to the difference in flux values shown in Table 1. Permeation flux was much lower than pure water flux at each curing time respectively.

Curing time does not linearly correlated well with xylose separation factor as illustrated in Fig. 3 (d). By ignoring the 15 minute point, a linear trend of decrease in performance can be observed as the membrane were exposed longer to the curing temperature. Similar results are reported for hexane-based TFC membranes formed with the different use aqueous monomer, coating conditions and support membrane [14,16].

Interestingly, a sudden surge of improvement in membrane performance at the 15 minute point shows further exposure to curing temperature after the minimum 5 minute point was needed to achieve higher separation performance. The increase in membrane hydrophilicity at 15 minute point as in Fig. 3 (a) would explain the improvement of membrane performance. Past studies [21,22] point out hydrophilic compounds such as xylose can easily pass through the membrane due to the hydrophilic-hydrophobic interaction between membrane and compounds. A commercial membrane with the better hydrophilic surface or lower contact angle also have been reported to have higher xylose separation factor [5,6].

Overall, the curing time has a large impact on TFC membrane surface hydrophilicity which affects the separation performance. The hydrophobic-hydrophilic interaction between TFC membranes dictated the separation between two almost similar compounds, xylose, and glucose. Also, TFC membranes expose to longer curing time have a decrease in flux. The decrease in flux is because of the resistance of membrane in allowing solutes to pass through, which may cause by a decrease in membrane pore size and porosity, and thickness of IP layer. TFC membrane with smaller pore size and porosity restricted the amount of solute to pass through them during filtration, which causes the flux to decrease. Blocking of pores by larger solutes further reduce the flux, which can be seen in permeation flux much lower than pure water flux at each curing time respectively. A thicker layer of IP make a solute travel longer distance through the membrane, is also a form of hindrance coming from the membrane. In all the events, the hydrophobic-hydrophilic interaction, pore size, porosity, and thickness of IP layer were the outcomes of IP reaction. The increase in curing time makes IP reaction more complete, this makes the polymer chain in IP layer to pack more closely. This causes the densification of IP layer, in turn

making the membrane less porous and thicker IP layer.

4. Conclusion

In conclusion, curing time do have an impact on the membrane hydrophilicity and performance of hexane-based TFC membrane. As the TFC membrane was subjected to longer exposure to curing, the top layer would become denser which decreases the flux of pure water and monosaccharides. The minimum time for hexane to be removed from the TFC membrane was at least 5 minutes, but 15 minutes of curing was needed to enhance the xylose separation at a curing temperature of 60 ºC. However, it should be noted the proper combination of curing time and temperature of the TFC membranes mentioned by [16] combine with proper preparative conditions [13,14] would further enhance the membrane performance.

5. Acknowledgements

The authors wish to express their thanks to Ministry of Education through the financial aid from grant RDU140901, LRGS/2013/UKM-UKM/PT/03, and RDU140336. The authors also wish to acknowledge the Ministry of Education Malaysia for sponsoring K.H. Mah postgraduate's study via MyBrain15 program.

6. Nomenclature

List of Abbreviation

ATR-FTIR	Attenuated Total Reflectance-Fourier Transform Infrared
FTIR	Fourier Transform Infrared
HPLC	High Performance Liquid Chromatography
IP	Interfacial Polymerization
PES	Polyethersulfone
TEOA	Triethanolamine
TFC	Thin-film composite
TMC	Tri-mesoyl chloride

List of Symbols

A	Effective membrane area (m^2)
C_b	Concentration of respective solute in bulk (g/100 g of solution)
$Cb_{\_glu}$	Concentration of glucose in the bulk (g/100 g of solution)
$Cb_{\_xyl}$	Concentration of xylose in the bulk (g/100 g of solution)
C_f	Concentration of respective solute in feed (g/100 g of solution)
Cp	Concentration of respective solute in permeate (g/100 g of solution)
$Cp_{\_glu}$	Concentration of glucose in permeate (g/100 g of solution)
$Cp_{\_xyl}$	Concentration of xylose in permeate (g/100 g of solution)
C_r	Concentration of respective solute in retentate (g/100 g of solution)
J_v	Permeation flux (L m-2 h-1)
J_w	Water flux (L m-2 h-1)
r	Correlation coefficient
R_{obs}	Observed retention of respective solute
Δt	measured period of time for collection of ultrapure water (h)
∇V	volume of ultrapure water collected (L)
X_{xyl}	xylose separation factor

References

[1] Ramaswamy S, Huang H, Ramarao B. *Separation and purification technologies in biorefineries.* United Kingdom: John Wiley & Sons, Ltd; 2013.

[2] da Silva SS, Chandel AK. *D-Xylitol: Fermentative Production, Application, and Commercialization.* Heidelberg: Springer; 2012.

[3] Zahari MAKM, Abdullah SSS, Roslan AM, Ariffin H, Shirai Y, Hassan MA. Efficient utilization of oil palm frond for bio-based products and biorefinery. *J Clean Prod* 2014;65:252–60.

[4] Hassan O, Ling TP, Maskat MY, Illias RM, Badri K, Jahim J, et al. Optimization of pretreatments for the hydrolysis of oil palm empty fruit bunch fiber (EFBF) using enzyme mixtures. *Biomass and Bioenergy* 2013;56:137–46.

[5] Sjoman E, Manttari M, Nystrom M, Koivikko H, Heikkila H. Separation of xylose from glucose by nanofiltration from concentrated monosaccharide solutions. *J Memb Sci* 2007;292:106–15.

[6] Sjöman E, Mänttäri M, Nyström M, Koivikko H, Heikkilä H. Xylose recovery by nanofiltration from different hemicellulose hydrolyzate feeds. *J Memb Sci* 2008;310:268–77.

[7] Morthensen ST, Luo J, Meyer AS, Jørgensen H, Pinelo M. High performance separation of xylose and glucose by enzyme assisted nanofiltration. *J Memb Sci* 2015;492:107–15.

[8] Lau WJ, Ismail AF, Misdan N, Kassim MA. A recent progress in thin film composite membrane: A review. *Desalination* 2012;287:190–9.

[9] Mohammad AW, Teow YH, Ang WL, Chung YT, Oatley-Radcliffe DL, Hilal N. Nanofiltration membranes review: Recent advances and future prospects. *Desalination* 2015;356:226–54.

[10] Lau WJ, Ismail AF. Progress in interfacial polymerization technique on composite membrane preparation. 2nd Int. Conf. Environ. Eng. Appl. 2011:173–7.

[11] Hilal N, Khayet M, Wright CJ. *Membrane modification: Technology and applications.* Florida, USA: CRC Press, Taylor & Francis Group; 2012.

[12] Tang B, Huo Z, Wu P. Study on a novel polyester composite nanofiltration membrane by interfacial polymerization of triethanolamine (TEOA) and trimesoyl chloride (TMC): I. Preparation, characterization and nanofiltration properties test of membrane. *J Memb Sci* 2008;320:198–205.

[13] Ghosh AK, Jeong B-H, Huang X, Hoek EMV. Impacts of reaction and curing conditions on polyamide composite reverse osmosis membrane properties. *J Memb Sci* 2008;311:34–45.

[14] Prakash Rao A, Desai NV, Rangarajan R. Interfacially synthesized thin film composite RO membranes for seawater desalination. *J Memb Sci* 1997;124:263–72.

[15] Zhao J, Wang Z, Wang J, Wang S. Influence of heat-treatment on CO2 separation performance of novel fixed carrier composite membranes prepared by interfacial polymerization. *J Memb Sci* 2006;283:346–56.

[16] Rangarajan R, Desai NV, Daga SL, Joshi SV, Prakash Rao A, Shah VJ, et al. Thin film composite reverse osmosis membrane development and scale up at CSMCRI, Bhavnagar. *Desalination* 2011;282:68–77.

[17] Prakash Rao A, Joshi S., Trivedi J., Devmurari C., Shah V. Structure–performance correlation of polyamide thin film composite membranes: effect of coating conditions on film formation. *J Memb Sci* 2003;211:13–24.

[18] Jalanni NA, Abu Seman MN, Faizal CKM. Investigation of New Polyester Nanofiltration (NF) Membrane Fouling with Humic Acid Solution. *J Teknol* 2013;65:69–72.

[19] Mah KH, Yussof HW, Jalanni NA, Seman MNA, ol N. Separation of Xylose From Glucose Using Thin Film Composite (TFC) Nanofiltration Membrane: Effect of Pressure, Total Sugar Concentration and Xylose/Glucose Ratio. *J Teknol* 2014;70:93–8.

[20] Tang B, Zou C, Wu P. Study on a novel polyester composite nanofiltration membrane by interfacial polymerization. II. The role of lithium bromide in the performance and formation of composite membrane. *J Memb Sci* 2010;365:276–85.

[21] Boussu K, Vandecasteele C, der Bruggen B. Relation between membrane characteristics and performance in nanofiltration. *J Memb Sci* 2008;310:51–65.

[22] Braeken L, Ramaekers R, Zhang Y, Maes G, Van Der Bruggen B, Vandecasteele C. Influence of hydrophobicity on retention in nanofiltration of aqueous solutions containing organic compounds. *J Memb Sci* 2005;252:195–203.